Robotica (2015) volume 33, pp. 1314–1324. © Cambridge University Press 2014
doi:10.1017/S0263574714000745

Control of a compass gait walker based on energy regulation using ankle push-off and foot placement

Pranav A. Bhounsule*

Disney Research Pittsburgh, Pittsburgh, PA 15213, USA

(Accepted February 24, 2014. First published online: April 1, 2014)

SUMMARY
In this paper, we present a theoretical study on the control of a compass gait walker using energy regulation between steps. We use a return map to relate the mid-stance robot kinetic energy between steps with two control inputs, namely, foot placement and ankle push-off. We show that by regulating robot kinetic energy between steps using the two control inputs, we are able to (1) generate a wide range of walking speeds and stride lengths, including average human walking; (2) cancel the effect of external disturbance fully in a single step (dead-beat control); and (3) switch from one periodic gait to another in a single step. We hope that insights from this control methodology can help develop robust controllers for practical bipedal robots.

KEYWORDS: Bipeds; Legged robots; Motion planning; Humanoid robots; Control of robotic systems.

1. Introduction

Current research on bipedal robots has focussed on planning and control of a singe steady state (periodic) walking gait. We characterize a walking gait by a given combination of step length and step velocity. However, for bipedal robots, to be able to walk in man-made environments, they need to be able to walk at a wide range of steady state periodic gaits and be able to switch from one periodic gait to another quickly.

In this paper, we show theoretical calculations on how to use energy regulation between steps to plan and control walking of a compass gait model. We first review past work on compass gait models and common control approaches, followed by a discussion on our model.

2. Related Works

2.1. Compass gait model

McGeer[1] was the first to demonstrate that a compass gait model, with properly tuned mechanics, can descend down gentle slopes without any control or energy input. This passive compass gait model has demonstrated a limited range of walking motions (usually slow speeds when compared with humans) and limited stability.[2,3] However, the biggest limitation of the passive compass gait model is that it cannot sustain steady walking on level ground because there is no means of supplying the energy lost during foot collision.

There have been attempts made to mimic passive compass gait motion on level ground by adding actuation. Asano *et al.*[4] simulated a virtual gravity field using robot actuators, which mimics the gravity field observed in slope walkers. Goswami *et al.*[5] and Spong[6] observed that the total energy of the passive compass gait model descending a slope is constant. Based on this observation, they developed a control scheme that uses the robot actuators to track a virtual energy field. Both, virtual gravity and energy-based control approaches, assume that the hip as well as the ankles are actuated

* Corresponding author. E-mail: pab47@disneyresearch.com

https://doi.org/10.1017/S0263574714000745 Published online by Cambridge University Press

(also called full actuation). However, assuming ankle actuation might be an unrealistic assumption because using too much ankle actuation during single stance can lead to overturning of the robot foot, violating the condition that the foot is firmly grounded. In this paper, our model has under-actuation for most of the stance phase, except during support transfer, where the trailing ankle applies an impulsive push-off.[7] Since ankle actuation in our model occurs at the end of single stance phase, that is, when the stance leg is about to become the new swing leg, foot overturning is not an issue.

2.2. Foot placement control

Use of foot placement for control is an old idea. Pratt *et al.*[8] used a "Capture point" analysis to investigate balance using foot placement. Capture point is the point where the robot should step to come to a complete stop when pushed. In their analysis, the capture point is computed using the zero of the orbital energy of the linear inverted pendulum model with collision-free support transfer.[9] Wight *et al.*[10] developed the "foot placement estimator" identical to the capture point concept. However, they used the compass gait model similar to the one we use.

2.3. Push-off control

Use of push-off for control is a relatively new idea, although, biomechanists have used it to explain mechanics of human walking. Kuo[11] used the compass gait model with impulsive ankle push-off to explain the energetics of human walking, and the preferred speed–step length relationship in human walking.[12] The timing of the push-off is critical for energy-efficiency; push-off before heel-strike is four times more energy-efficient than push-off after heel strike.[12,13] This is because a push-off before heel-strike tends to soften the collisional losses associated with the velocity re-direction during support transfer.[14] In this paper, we will use an ankle push-off before heel-strike. However, note that the equations of motion for support transfer (see Eq. (5)) for our model remain the same irrespective of whether the push-off is before or after heel-strike, although the energetics differ.

2.4. Compass gait model used in this paper

Our compass gait model has massless legs and a point-mass at the hip. We use a hip actuator to do foot placement, and an ankle actuator to do an impulsive push-off just before heel-strike. For practical robots, impulsive push-off is not possible because actuators cannot generate infinite forces. However, one can approximate the impulsive push-off with finite force over finite interval of time. For robots with knees, one can use knee actuator to generate the push-off.

We have used ideas from this model to develop an event-based feedback controller to regulate steady state walking for Cornell Ranger robot,[15] leading to a long distance walking record and energy-efficiency record.[16,17] However, that study was limited to planning and control of one steady state gait. Here we extend that study further. Using theoretical and numerical calculations, we demonstrate that it is possible for the compass gait model to generate wide range of speeds and step lengths, using a combination of foot placement and ankle push-off. We also show that by using the same two controls to do once-per-step energy regulation, we can stabilize a periodic gait and switch from one periodic gait to another in a single step.

3. The Compass Gait Model

Figure 1 shows our two-dimensional (2D) model of walking. The model has massless legs, each of length (ℓ) and a point-mass (M) at the hips. Gravity (g) points downwards as shown. The model has two actuators: a rotational hip actuator and a linear stance leg actuator on each leg. We assume that the hip actuator can place the swing leg at the desired position instantaneously, and the stance leg linear actuator generates an impulsive push-off along the stance leg. We assume perfect state estimation, no saturation limits on actuators, ignore swing leg dynamics (since the legs are massless), and assume that the grounded leg does not slip.

Figure 2 shows a typical step for this model. The point-mass model starts in the mid-stance position as shown in (I) with a stance leg velocity of $\dot{\theta}_i^m$. The model then moves passively to the state just before heel-strike in (b), where the stance leg velocity is $\dot{\theta}_i^-$. Next, the linear actuator on the stance leg applies an impulsive push-off (P_i) just before heel-strike (we assume that the point-mass does not takeoff during the impulsive push-off and this assumption is somewhat justified because the push-off

https://doi.org/10.1017/S0263574714000745 Published online by Cambridge University Press

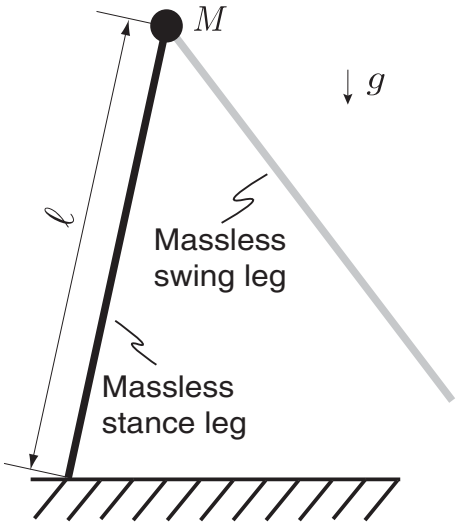


Fig. 1. 2D point-mass walker. The walker consists of two massless legs of length ℓ with a point-mass M at the hip joint. The leg on the ground is the stance leg and is shown in black, and the leg in the air is the swing leg and is shown in gray. Throughout the paper we assume that at least one leg is on the ground (single stance phase) and at no instance are both legs on the ground (no double stance phase). The support exchange, called heel-strike, is instantaneous.

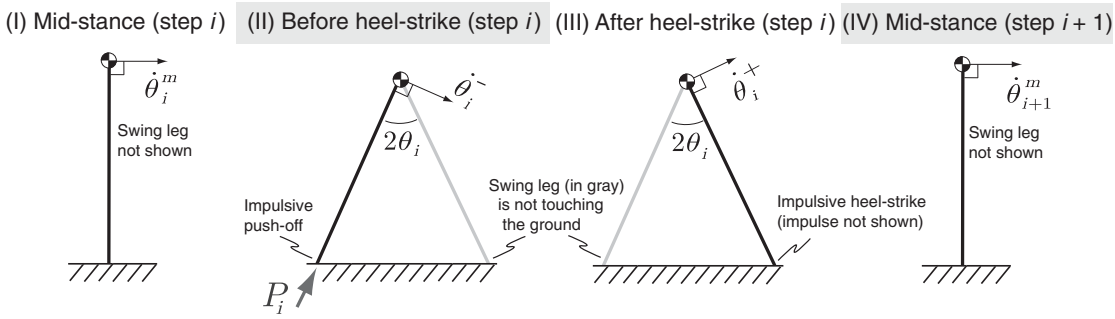


Fig. 2. A typical step of our point-mass model. The walker starts in the upright or mid-stance position in (I). Next, just before heel-strike in (II), the stance leg applies an impulsive push-off P_i and the hip actuator positions the swing leg at an angle $2\theta_i$. Next, after heel-strike in (III), the swing leg becomes the new stance leg. Finally, the walker ends up in the upright position or mid-stance position at the next step in (IV). Note that model moves passively from (I) to (II) and from (III) to (IV). The push-off impulse at (II) and the heel-strike impulse at (III) (heel-strike impulse is not shown) serve to redirect the point-mass from one circular arc to the next one. Note that the angular velocity is always perpendicular to the stance leg at all instances of time.

is immediately followed by heel-strike in (III)) and the hip actuator positions the swing leg at the angle $2\theta_i$. Next, in (III) the swing leg collides with the ground and becomes the new stance leg. The stance leg velocity after collision is $\dot{\theta}_i^+$. Finally, the new stance leg moves passively to the state (IV) where the model ends up in the mid-stance position with a stance velocity of $\dot{\theta}_{i+1}^m$.

4. Equations of Motion

We present equations of motion for a typical step shown in Fig. 2. Later, we will use these equations for gait planning and control.

4.1. Mid-stance position at step i (Fig. 2 (I)) to instant before heel-strike at step i (Fig. 2 (II))

The non-dimensional mid-stance velocity at step i is $\dot{\theta}_i^m$. Time is non-dimensionalized with $\sqrt{\ell/g}$ in all variables that have a time dependency. The inter leg angle at heel-strike is $2\theta_i$ and the stance leg

https://doi.org/10.1017/S0263574714000745 Published online by Cambridge University Press

velocity just before heel-strike is $\dot{\theta}_i^-$. Using conservation of energy we get,

$$\frac{\left(\dot{\theta}_i^m\right)^2}{2} + 1 = \frac{\left(\dot{\theta}_i^-\right)^2}{2} + \cos\theta_i. \tag{1}$$

We use force balance along the stance leg to derive an expression for the net ground reaction force, F (non-dimensionalized with Mg). Further, to prevent tensional leg forces, the net reaction force should always be positive by our sign convention, and thus

$$F = \cos\theta - \dot{\theta}^2 > 0. \tag{2}$$

The angular speed $\dot{\theta}_i$ increases monotonically with the angle θ_i. Thus, we check for the condition given by Eq. (2) only during heel-strike (i.e., when the vertical angle is at its maximum). Furthermore, we can express this in terms of mid-stance velocity $\dot{\theta}_i^m$ using Eq. (1) to get

$$\begin{aligned} \cos\theta_i &> \left(\dot{\theta}_i^-\right)^2 \\ &> \left(\dot{\theta}_i^m\right)^2 + 2(1 - \cos\theta_i). \end{aligned} \tag{3}$$

Finally, we compute the time it takes to move from mid-stance position to the instant just before heel-strike. This is useful for computing the step time later. The time needed to move the first half step is

$$T_{\text{first half}} = \int_0^{\theta_i} \frac{d\theta}{\dot{\theta}} = \int_0^{\theta_i} \frac{d\theta}{\sqrt{\left(\dot{\theta}_i^m\right)^2 + 2(1 - \cos\theta)}}, \tag{4}$$

which we solve using numerical quadrature.

4.2. Instant before heel-strike at step i (Fig. 2 (II)) to instant after heel-strike at step i (Fig. 2 (III))
To relate angular velocities before heel-strike $\dot{\theta}_i^-$ to that after heel-strike $\dot{\theta}_i^+$, we do an angular momentum balance about the impending collision point (see refs [11, 13] for more details on this calculation). Using the non-dimensional impulsive push-off P_i (non-dimensionalized with $M\sqrt{g\ell}$), we get

$$\dot{\theta}_i^+ = P_i \sin 2\theta_i + \dot{\theta}_i^- \cos 2\theta_i. \tag{5}$$

4.3. Instant after heel-strike at step i (Fig. 2 (III)) to mid-stance position at step i + 1 (Fig. 2 (IV))
Let the mid-stance velocity at step $i + 1$ be $\dot{\theta}_{i+1}^m$. Using conservation of energy we get,

$$\frac{\left(\dot{\theta}_i^+\right)^2}{2} + \cos\theta_i = \frac{\left(\dot{\theta}_{i+1}^m\right)^2}{2} + 1. \tag{6}$$

We also need to ensure that the ground reaction force is positive. We do this using the same procedure used to derive Eq. (3). Thus,

$$\begin{aligned} \cos\theta_i &> \left(\dot{\theta}_i^+\right)^2 \\ &> \left(\dot{\theta}_{i+1}^m\right)^2 + 2(1 - \cos\theta_i). \end{aligned} \tag{7}$$

https://doi.org/10.1017/S0263574714000745 Published online by Cambridge University Press

We compute the time taken for the second half of the step as done earlier in Eq. (4). Thus,

$$T_{\text{second half}} = \int_0^{\theta_i} \frac{d\theta}{\dot{\theta}} = \int_0^{\theta_i} \frac{d\theta}{\sqrt{\left(\dot{\theta}_{i+1}^m\right)^2 + 2(1-\cos\theta)}}. \tag{8}$$

4.4. Step-to-step map for planning and control

We analyze the system using a Poincaré map from one mid-stance to the next. We relate the stance leg velocity at mid-stance at step i with that at mid-stance at step $i+1$. Putting Eqs. (1) and (6) in Eq. (5) and solving for $\dot{\theta}_{i+1}^m$ gives

$$\begin{aligned}\dot{\theta}_{i+1}^m &= f(\dot{\theta}_i^m, \theta_i, P_i) \\ &= \left\{ \left(P_i \sin 2\theta_i + \sqrt{(\dot{\theta}_i^m)^2 + 2(1-\cos\theta_i)}\cos 2\theta_i \right)^2 - 2(1-\cos\theta_i) \right\}^{1/2}.\end{aligned} \tag{9}$$

The above expression relates the mid-stance velocity at step $i+1$ as a function of mid-stance velocity at step i and the two control variables: inter-leg angle at heel-strike ($2\theta_i$), and impulse (P_i). We use this equation for gait planning and control. Note that we also have to ensure that inequalities given by Eqs. (3) and (7) are satisfied.

4.5. Step length, step time, and step velocity

We compute the non-dimensional step length, D_i (non-dimensionalized by ℓ) from the inter-leg angle at heel-strike as follows:

$$D_i = 2\sin\theta_i. \tag{10}$$

We calculate the total non-dimensional step time, T_i, by adding Eqs. (4) and (8)

$$T_i = T_{\text{first half}} + T_{\text{second half}}. \tag{11}$$

Finally, we compute the non-dimensional step velocity, V_i, from the non-dimensional step length and non-dimensional step time,

$$V_i = \frac{D_i}{T_i}. \tag{12}$$

5. Results

5.1. Planning a steady state (periodic) walk

In periodic walking, the stance leg velocity at mid-stance at step $i+1$ is the same as the stance leg velocity at mid-stance at step i. Thus, we set $\dot{\theta}_{i+1}^m = \dot{\theta}_i^m = \dot{\theta}_0^m$ (steady state mid-stance hip velocity), $P_i = P_0$ (steady state impulse), and $\theta_i = \theta_0$ (steady state half inter-leg angle at heel-strike) in Eq. (9). This gives one equation in three variables (P_0, θ_0, and $\dot{\theta}_0^m$). We are free to choose two of the three variables to characterize the steady state gait.

We choose to quantify a steady state gait by the half inter-leg angle at heel-strike, θ_0, and mid-stance velocity, $\dot{\theta}_0^m$. We can now solve for the steady state impulse P_0 from Eq. (9) as a function of θ_0 and $\dot{\theta}_0^m$ to get

$$P_0 = \tan\theta_0 \sqrt{\left(\dot{\theta}_0^m\right)^2 + 2(1-\cos\theta_0)}. \tag{13}$$

We present results for a typical human gait. The nominal human velocity is $v_0 = 1.3$ m/s.[18] We convert this into non-dimensional form, $V_0 = v_0/\sqrt{g\ell} = 1.3/\sqrt{10\times 1} = 0.41$. To get the step length,

https://doi.org/10.1017/S0263574714000745 Published online by Cambridge University Press

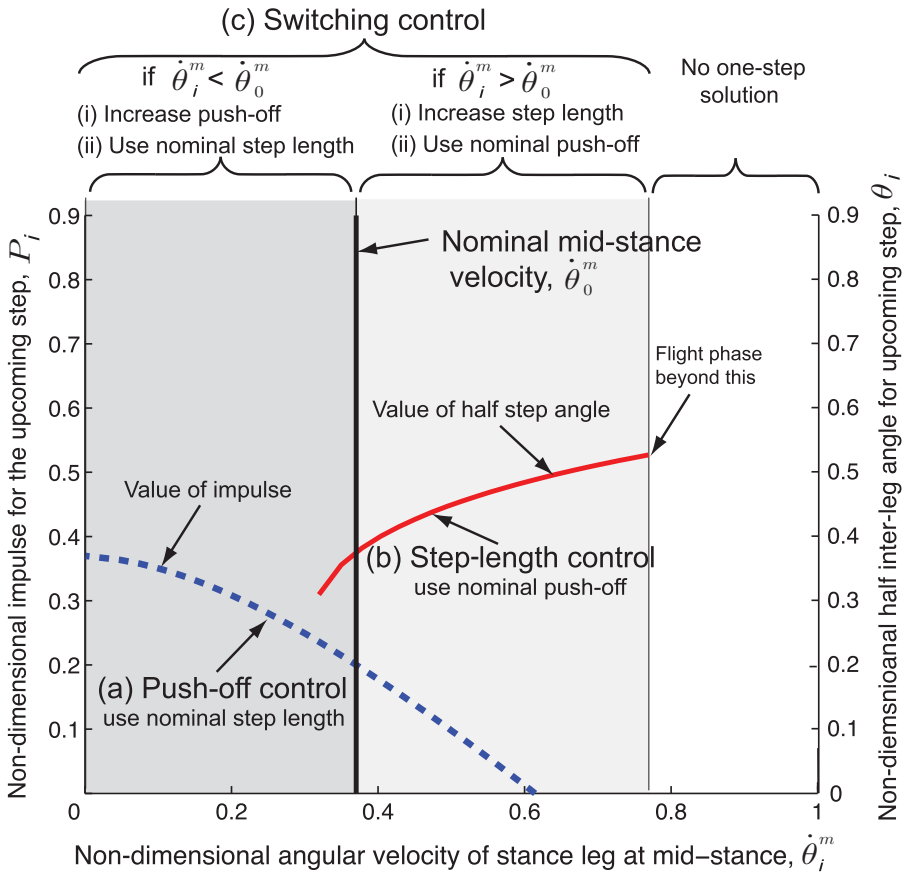


Fig. 3. Three strategies to control steady state walking. (a) Push-off control with step length maintained at the nominal value (blue dashed line). Push-off control works best to inject energy and to speed up the system. (b) Step length control with push-off maintained at the nominal value (red solid line). Step length control works best to extract energy and to slow down the system. (c) Switching between push-off and step length control based on velocity at mid-stance. If the mid-stance velocity is less than the nominal value, then a push-off control is used to inject energy to speed up the system (blue dashed line in the gray region). If the mid-stance velocity is more than the nominal value, then a step-length control is used to extract excess energy to slow down the system (red solid line in gray region). Such a controller is simple to program and works in all mid-stance velocity regimes except for too high velocities (white region on the right side) where we either need a flight phase to do a one-step control or would need multiple walking steps to get back to the nominal speed.

we use the empirical fit by Alexander and Maloiy,[19] $D_0 = 1.25 \times V_0^{0.6} = 1.25 \times 0.41^{0.6} = 0.73$. Using the values for D_0 and V_0 in Eq. (12), the non-dimensional step time is $T_0 = 1.78$. These values will be used later in Section 5.2.

We substitute the value of D_0 in Eq. (10) and compute the inter-leg angle at heel-strike. We get $2\theta_0 = 0.7508$. Next, using the computed values of θ_0 and T_0 in Eq. (11), we compute the mid-stance velocity. We get $\dot{\theta}_0^m = 0.3702$. Finally, putting the values of $\dot{\theta}_0^m$ and θ_0 in Eq. (13) gives the impulse, $P_0 = 0.2072$.

5.2. Range of solutions

Next, we will find all the possible steady state gaits possible with this model. A solution is feasible if the ground reaction force is positive during stance phase. To compute the boundary of feasible solutions we put $\theta_i^m = \theta_0$ and $\dot{\theta}_i^m = \dot{\theta}_0^m$ and use Eqs. (3) or (7) to compute a relation between θ_0 and $\dot{\theta}_0^m$. All the feasible walking solutions should satisfy the constraint

$$\cos\theta_0 < \frac{\left(\dot{\theta}_0^m\right)^2 + 2}{3}. \tag{14}$$

https://doi.org/10.1017/S0263574714000745 Published online by Cambridge University Press

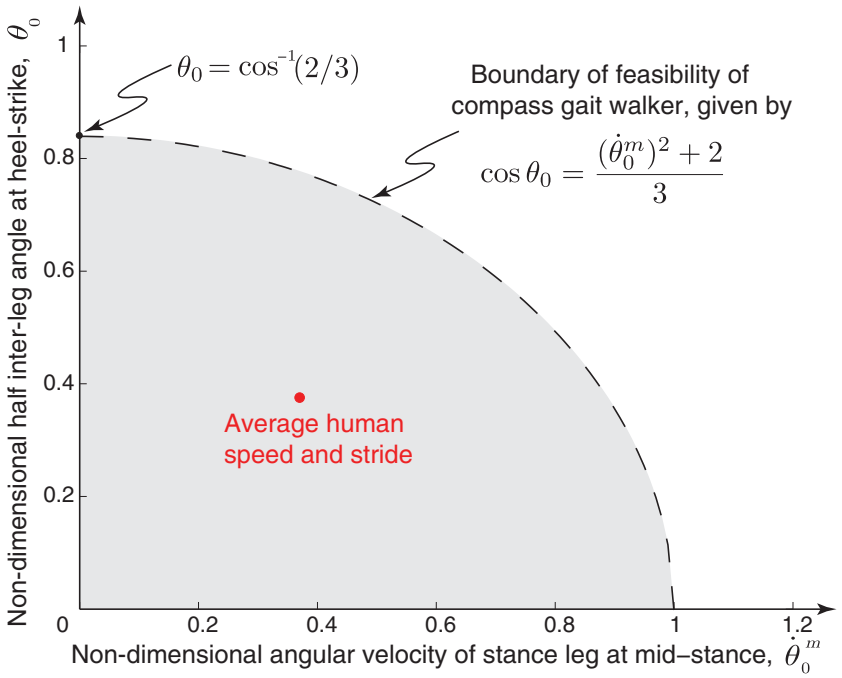


Fig. 4. Range of steady state solutions possible with the compass gait model. The gray region shows the feasible region of walking. The boundary of the feasible regions is given by the equality in Eq. (14).

The grey shaded region in Fig. 4 shows the feasible region of walking obtained from Eq. (14). We have also plotted the average human walking obtained from Section 5.1.

5.3. Controlling steady state (periodic) walk

Next, we consider how to recover from external disturbances to get back to the periodic walking gait. We model the effect of external disturbance as a change in stance leg velocity at mid-stance. Thus, given a measured change in mid-stance velocity at step i, we want to find what control strategy will get the model back to the nominal mid-stance velocity at step $i + 1$.

We use the Poincaré map[20] from one mid-stance (instance of time when the stance leg is vertical) to another for control and is given by Eq. (9). We use the measured stance leg velocity at mid-stance to compute a foot placement and a push-off impulse so as to return to the steady state mid-stance velocity at the next step. Such a strategy that involves full correction of disturbance in one step is called a one-step dead-beat control.[21] Instead, we could have designed a strategy that does a full correction of disturbance in n steps, also called n-step dead-beat control. This is useful when a single step dead-beat is not possible due to actuator limits. Dead-beat control of running has been studied by Carver *et al.*[22] and Wu and Geyer.[23]

In summary, our control problem is as follows: Given that the mid-stance velocity is different from the nominal due to a disturbance, i.e., $\dot{\theta}_i^m \neq \dot{\theta}_0^m$; we need to find a control law (a value of P_i and θ_i) that gets the robot back to the steady state values $\dot{\theta}_0^m$ at the mid-stance of the next step.

In the discussion that follows, we use the term step length and inter-leg angle at heel-strike interchangeably. We present results for the steady state human walking gait that we computed in Section 5.1.

5.3.1. Push-off control. One simple approach is to fix the step length to the nominal value, i.e., $2\theta_0$, and adjust the impulse. We call this approach the push-off control approach. In Eq. (9), we vary the mid-stance velocity at mid-stance at step i, $\dot{\theta}_i^m$, to simulate a disturbance, and try to find the impulse P_i such that $\dot{\theta}_{i+1}^m = \dot{\theta}_0^m$ and with $\theta_i = \theta_0$ to generate the dashed blue line in Fig. 3. From the plots, we see that there is an impulse for all velocities slower than nominal, $\dot{\theta}_i^m < \dot{\theta}_0^m$. However, we are not able to find a nonzero impulse solution for certain range in the faster than nominal velocities regime $\dot{\theta}_i^m > \dot{\theta}_0^m$. Note that a negative impulse implies a tensional leg force, which is not physically possible.

https://doi.org/10.1017/S0263574714000745 Published online by Cambridge University Press

From this plot, we conclude that push-off control works best to speed up the system (or increase the robot's kinetic energy).

5.3.2. Step-length control. Another simple approach is to fix the impulse to the nominal value, i.e., P_0, and adjust the step length. We call this approach the step-length control approach. In Eq. (9), we vary the mid-stance velocity at step i, $\dot{\theta}_i^m$, to simulate an external disturbance, and try to find a step length, $2\theta_i$, such that with $P_i = P_0$, $\dot{\theta}_{i+1}^m = \dot{\theta}_0^m$, resulting in the solid red line in Fig. 3. We obtain the boundary of the solid red line in the high-speed region by checking the take-off condition given by Eq. (3).

From this plot, we see that there is a step length for the velocities faster than nominal, $\dot{\theta}_i^m > \dot{\theta}_0^m$ except to the far right where the solid red line ends. In this region, the robot needs a flight phase to do a one-step dead beat control. Also, note we are not able to find a step length for most of the region in the slower than nominal velocities range, i.e., $\dot{\theta}_i^m < \dot{\theta}_0^m$. In this region, the robot falls backward before it can make it to the top at the next step. Thus, the step length control works best to slow down the system (or decrease the robot's kinetic energy). This is because by changing the step length one is effectively changing the energy losses at heel-strike. For a given impulse, a big step implies a bigger loss and *vice versa* for a small step.[13]

5.3.3. Two one-sided controllers—switching between push-off control and step-length control in different mid-stance velocity regimes. Informed by the results in the above two sections, we note that the push-off control works best to speed up the system and the step length control works best to slow down the system. Hence, we propose two one-sided controllers as follows: If the mid-stance velocity of the system is less than the steady state value, i.e., $\dot{\theta}_i^m < \dot{\theta}_0^m$, we use a push-off control; and if the mid-stance velocity of the system is more than the steady state value, i.e., $\dot{\theta}_i^m > \dot{\theta}_0^m$, we use the step length control. The highlighted gray regions in Fig. 3 shows the switching controller. Saglam and Byl[24] used a switching controller that does approximately the same as we have done here.

However, there exists a range of non-dimensional mid-stance velocities between 0.78 and 1, where we cannot cancel the effect of disturbances in a single walking step. In this region, we need a flight phase for one-step correction or need more than one step to get back to the steady state gait.

We have used a similar switching controller to regulate the speed of the walking robot Cornell Ranger,[16] leading to long-distance walking record.

5.4. One-step transition from one periodic gait to another

We want to find out if it is possible to switch from one periodic gait to another in one step. So we did the following. For a given combination of mid-stance velocities, $\dot{\theta}_i^m$ and $\dot{\theta}_{i+1}^m$, we try to find out if there is at least one combination of control parameters, θ_i and P_i. We do this by using a root finding algorithm. The gray region shown in Fig. 5 represents all the mid-stance velocity transitions possible in one step. This gray area is also called the one-step basin of attraction.[1]

The four edges that define the basin of attraction are: (i) $\dot{\theta}_i^m = 0$ (x-axis) corresponds to robot starting at the mid-stance position and is excluded because it takes infinite time to move from this position; (ii) $\dot{\theta}_{i+1}^m = 0$ (y-axis) corresponds to the robot ending up at the mid-stance position and is excluded because it takes infinite time to get to this position; (iii) for $\dot{\theta}_{i+1}^m = 1$ the normal force on the stance leg will go to zero at mid-stance by Eq. (7); and (iv) the fourth edge on the right side comes from excluding the solutions that violate Eq. (3).

One might wonder why the basin of attraction is not symmetric about the steady state walking solution (red dashed line with slope of 1). In the region below the steady state walking, the robot is going from a high velocity gait to a low velocity gait. To achieve this, the robot needs to slow down. This is best achieved by taking a big step, but too big a step violates the condition that the reaction force on the stance leg should be positive (see Eq. (3)), leading to nonexistence of solutions. On the other hand, for the region above steady state walking, the robot is going from a low velocity gait to a high velocity gait. To achieve this, the robot needs to speed up. This is best achieved by increasing the push-off. But it is always possible to find a value of push-off impulse with a suitably sized step length to speed up the system without violating the take-off condition given by Eq. (7).

[1] For a dynamical system with a periodic orbit, the basin of attraction is defined as the set of initial conditions from which the system will return to the periodic orbit.

https://doi.org/10.1017/S0263574714000745 Published online by Cambridge University Press

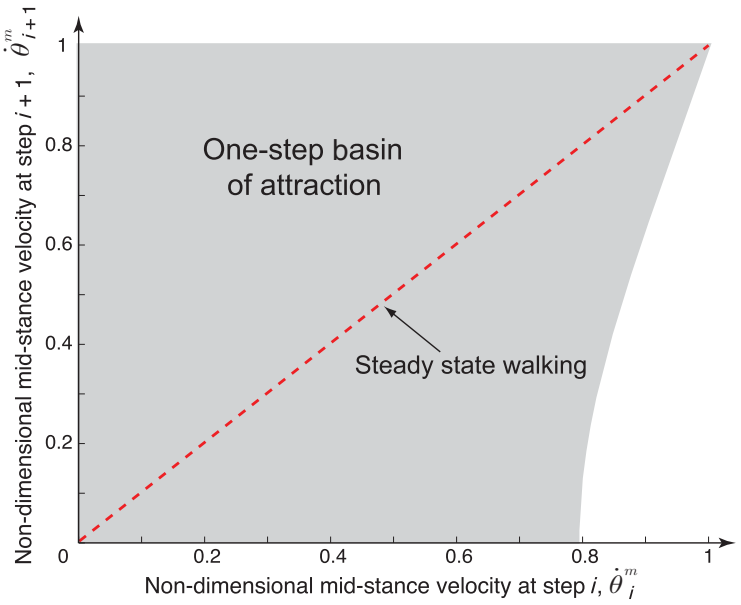


Fig. 5. One-step basin of attraction The gray area is the region where we can find at least one combination of θ_i and P_i to transition from two given mid-stance velocities, $\dot{\theta}^m_i$ to $\dot{\theta}^m_{i+1}$. Steady (periodic) walking is shown as a red dashed line. The slope of this line is 1.

Note that the top and right boundaries of the one-step basin of attraction are limitations imposed by our assumption that running is not permitted.

5.5. Balance control via capture point

The capture point is defined as the point where the robot should step to come to a complete stop when pushed.[8] If the robot comes to complete stop in one step, it is called a one-step capture point.

We compute the one-step capture point as follows. We put $P_i = 0$ and $\dot{\theta}^m_{i+1} = 0$ in Eq. (9) and solve for the step length, $2\theta_i$, for the given disturbance characterized by $\dot{\theta}^m_i$. We show a plot of the one-step capture point in Fig. 6. There is no solution when the reaction force on the stance leg goes to zero and found by checking Eq. (3). However, if we allow flight phase, the solution is unbounded.

6. Conclusions and Future Work

In this paper, we presented a theoretical study on gait planning and control of bipedal walking using the compass gait model. In our compass gait model, the legs are massless and there is a point-mass at the hip. The point-mass vaults over the stance leg passively throughout the stance phase except during support transfer, in which the trailing leg applies an impulsive push-off followed by instantaneous collisional heel-strike during foot placement. We analytically derive return map that relates the stance leg velocity at mid-stance (instance when the stance leg is parallel to the gravity vector) as a function of stance leg velocity at the previous mid-stance and the two control inputs, namely, the foot placement and the push-off impulse. We then show how to use the map to plan and control a periodic walking gait and to transition from one periodic gait to another. The central idea for control in this approach is to regulate the kinetic energy from step to step using push-off and foot placement. Our key results are as follows: (1) We can generate a wide range of walking speeds and stride lengths, including average human walking. (2) To stabilize a periodic motion when perturbed, a strategy which switches between push-off control and foot placement control gives the widest range of disturbance rejection than a single strategy. (3) It is possible to switch from one steady state gait to another in one step using a combination of push-off control and foot placement control.

This study raises some issues for the future work. We focus on one-step control entirely, but sometimes it might not be possible to do one-step control because of actuator limits (e.g., torque saturation, maximum acceleration). These limits impose bounds on how much push-off is possible

https://doi.org/10.1017/S0263574714000745 Published online by Cambridge University Press

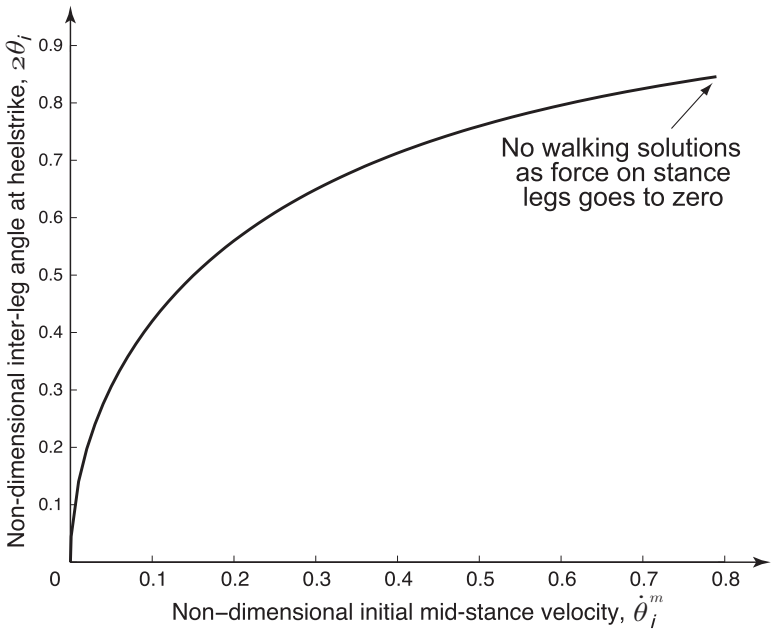


Fig. 6. One step capture point. The external disturbance is modeled as a nonzero mid-stance velocity (x-axis). The plot shows the step length (y-axis) needed for the robot to come to a complete stop (zero mid-stance velocity of the stance leg) at the next mid-stance. For high enough velocities, there are no solutions because the reaction force on the stance leg goes to zero. If we allow for a flight phase, the solution is unbounded.

and how fast the legs can swing. In these instances, a multiple step control strategy can be used. It would be interesting to understand multiple step control strategy in the context of actuator limits.

We have explored a range of motions and robustness of walking, but have ignored the cost of control.[25] For example, the choice of push-off control or step-length control can be based on energetic or actuator cost. Also, it would be interesting to understand the tradeoff between control cost and performance cost for single-step and multi-step strategies.

Acknowledgment

The author would like to thank Andy Ruina for initial discussions on the ideas presented here and an anonymous reviewer for insightful comments that shaped the writing of this manuscript. Wouter Wolfslag independently did most of the calculations presented here and gave the idea for Fig. 5. About half of the work was done when the author was a student at Cornell University.

References

1. T. McGeer, "Passive dynamic walking" *Int. J. Robot. Res.* **9**(2), 62–82 (1990).
2. M. Garcia, A. Chatterjee, A. Ruina and M. Coleman, "The simplest walking model: Stability, complexity, and scaling," *J. Biomech. Eng.* **120**(2), 281–288 (1998).
3. A. Goswami, B. Thuilot and B. Espiau, "A study of the passive gait of a compass-like biped robot symmetry and chaos," *Int. J. Robot. Res.* **17**(12), 1282–1301 (1998).
4. F. Asano, M. Yamakita and K. Furuta, "Virtual Passive Dynamic Walking and Energy-Based Control Laws" *International Conference on Intelligent Robots and Systems*, Takamatsu, Japan (Oct. 30–Nov. 5, 2000) pp. 1149–1154.
5. A. Goswami, B. Espiau and A. Keramane, "Limit cycles in a passive compass gait biped and passivity-mimicking control laws," *Auton. Robots* **4**(3), 273–286 (1997).
6. M. W. Spong, "Passivity Based Control of the Compass Gait Biped," *Proceedings of IFAC World Congress*, Beijing, China (Jul. 5–9, 1999) pp. 19–24.
7. K. Byl and R. Tedrake. "Approximate Optimal Control of the Compass Gait on Rough Terrain," *International Conference on Robotics and Automation*, Pasadena, California (May 19–23, 2008) pp. 1258–1263.
8. J. Pratt, J. Carff, S. Drakunov and A. Goswami, "Capture Point: A Step Toward Humanoid Push Recovery," *International Conference on Humanoid Robots*, Genova, Italy (Dec. 4–6, 2006) pp. 200–207.

https://doi.org/10.1017/S0263574714000745 Published online by Cambridge University Press

9. S. Kajita and K. Tani, "Experimental Study of Biped Dynamic Walking in the Linear Inverted Pendulum Mode," **In:** *International Conference on Robotics and Automation*, Nagoya, Aichi, Japan (May 21–27, 1995) pp. 2885–2891.
10. D. L. Wight, E. G. Kubica and D. W. Wang, "Introduction of the foot placement estimator: A dynamic measure of balance for bipedal robotics," *J. Comput. Nonlinear Dyn.* **3**(1), 011 009–1:10 (2008).
11. A. D. Kuo, "Energetics of actively powered locomotion using the simplest walking model," *J. Biomech. Eng.* **124**(1), 113–120 (2002).
12. A. D. Kuo, "A simple model of bipedal walking predicts the preferred speed–step length relationship," *J. Biomech. Eng.* **123**, 264–269 (2001).
13. A. Ruina, J. E. Bertram and M. Srinivasan, "A collisional model of the energetic cost of support work qualitatively explains leg sequencing in walking and galloping, pseudo-elastic leg behavior in running and the walk-to-run transition," *J. Theor. Biol.* **237**(2), 170–192 (2005).
14. A. D. Kuo and J. M. Donelan, "Dynamic principles of gait and their clinical implications," *Phys. Ther.* **90**(2), 157–174 (2010).
15. P. A. Bhounsule, A Controller Design Framework for Bipedal Robots: Trajectory Optimization and Event-Based Stabilization *Ph.D. Thesis*, Cornell University, Ithaca, NY (2012).
16. P. A. Bhounsule, J. Cortell, A. Grewal, B. Hendriksen, J. G. D. Karrsen, C. Paul and A. Ruina, "Low-bandwidth reflex-based control for lower power walking: 65 km on a single battery charge," *Int. J. Robot. Res.* (in press).
17. A. Ruina, "Cornell ranger 2011, 4-legged bipedal robot. Available at: http://ruina.tam.cornell.edu/research/topics/locomotion_and_robotics/rang er/Ranger2011/ (2013, June), online. (Or Google search for Cornell ranger).
18. H. J. Ralston, "Energy–speed relation and optimal speed during level walking," *Int. Zeitschrift für angewandte Physiologie einschließlich Arbeitsphysiologie* **17**(4), 277–283 (1958).
19. R. Alexander and G. M. O. Maloiy, "Stride lengths and stride frequencies of primates," *J. Zoology* **202**(4), 577–582 (1984).
20. S. Strogatz, *Nonlinear Dynamics and Chaos: With Applications to Physics, Biology, Chemistry and Engineering* (Perseus Books, New York, NY, 2001).
21. P. J. Antsaklis and A. N. Michel, *Linear Systems* (Birkhauser, Boston, MA, 1997).
22. S. G. Carver, N. J. Cowan and J. M. Guckenheimer, "Lateral stability of the spring-mass hopper suggests a two-step control strategy for running," *Chaos Interdiscip. J. Nonlinear Sci.* **19**(2), 026106–026106 (2009).
23. A. Wu and H. Geyer, "The 3-D spring–mass model reveals a time-based deadbeat control for highly robust running and steering in uncertain environments," *IEEE Trans. Robot.* **99**, 1–11 (2013).
24. C. O. Saglam and K. Byl, "Switching Policies for Metastable Walking," *International Conference on Decisions and Control*, Florence, Italy, (Dec. 10–13, 2013) pp. 977–983.
25. M. Srinivasan and A. Ruina, "Computer optimization of a minimal biped model discovers walking and running," *Nature* **439**(7072), 72–75 (2005).

https://doi.org/10.1017/S0263574714000745 Published online by Cambridge University Press